Microelectronics Reliability 154 (2024) 115337

Contents lists available at ScienceDirect

Microelectronics Reliability

journal homepage: www.elsevier.com/locate/microrel

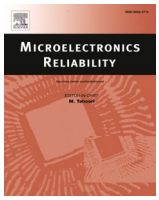

Research Paper

Effect of the loop forming process on the lifetime of aluminum heavy wire bonds under accelerated mechanical testing

Florens Felke [a,*], Anne Groth [b,c], Martin Hempel [c], Bernhard Czerny [d], Golta Khatibi [e], Torsten Döhler [a], Ute Geissler [a]

[a] TH Wildau, Hochschulring 1, 15745 Wildau, Germany
[b] TU Berlin, Straße des 17. Juni 135, 10623 Berlin, Germany
[c] Fraunhofer IZM, Gustav-Meyer-Allee 25, 13355 Berlin, Germany
[d] FH Burgenland, Campus 1, A-7000 Eisenstadt, Austria
[e] TU Vienna, Getreidemarkt 9/CT-164, 1060 Vienna, Austria

ARTICLE INFO

Keywords:
Aluminum heavy wire bonding
Mechanical accelerated lifetime testing method
Heel crack
Loop forming process
Wrinkling

ABSTRACT

Heavy wire bonding is one of the most common interconnection technologies in manufacturing of high-power electronics. For industrial applications, the long-term reliability of these connections is crucial. Besides the selection of the wire material and the loop geometry itself, the loop forming process parameters also have an influence on the reliability of the wire bond. In this work, the influence of the backward bond head movement during wire bonding process on the quality of wire bond connections was systematically investigated and qualified by cyclic mechanical lifetime tests, surface roughness measurements of the heel area by laser confocal microscopy and static pull tests. The wire bond loops were fabricated with 300 µm aluminum H11 and H14CR wires with different hardness values. The lifetime at low frequency cycle and high frequency cycle regime was determined by means of two different mechanical cyclic test methods operating at 5 Hz and at 60 kHz respectively. The results have shown, that the surface topology of the heel region caused by the initial plastic deformation during the loop forming process has a significant effect on the wire bond failure due to heel cracking. The number of loading cycles to failure shows an inverse correlation with the degree of surface roughness in a so called wrinkling analysis in the low and high frequency cycle regime. The soft wire exhibits different lifetimes compared to the hard ones depending on the testing conditions, while a significant decrease of the lifetime is observed with >30 % reverse movement during bonding in all cases.

Abbreviations

r. f.	reverse factor	%
Vvv	volume void valley	$\mu m^3/\mu m^2$
Vvc	volume void core	$\mu m^3/\mu m^2$
Vmc	volume material core	$\mu m^3/\mu m^2$
Vmp	volume material peak	$\mu m^3/\mu m^2$
n	number of measurements/sample size	–
BAMFIT	Bond accelerated mechanical fatigue interconnect testing	–
Δx	amplitude	µm
f	frequency	Hz
d	wire diameter	µm
LCT	loop cycle test	–
N_f	number of cycles until failure	–
FEA	finite element analysis	

1. Introduction

Heavy wire bonds of high purity Al, Al alloys and recently Cu are broadly used for interconnection in power electronic modules [1–3]. However, heel crack and wire bond lift-off failure modes are still considered to be the major lifetime limiting factors of the entire module. During the manufacturing process, the heel area is exposed to specific stresses due to its location at the transition from the bond contact to the loop [3,4] (as indicated in Figs. 1 and 2 a). On the one hand, the two parameters ultrasonic energy and bond force impact the heel during the bonding process, which in turn affects the grain structure and the local

* Corresponding author.
E-mail addresses: florens.felke@fkphysiktechnik.com (F. Felke), anne.groth@tu-berlin.de (A. Groth), martin.hempel@izm.fraunhofer.de (M. Hempel), Bernhard.Czerny@fh-burgenland.at (B. Czerny), golta.khatibi@tuwien.ac.at (G. Khatibi), torsten.doehler@th-wildau.de (T. Döhler), geissler@th-wildau.de (U. Geissler).

https://doi.org/10.1016/j.microrel.2024.115337
Received 11 November 2023; Received in revised form 4 January 2024; Accepted 29 January 2024
Available online 21 February 2024

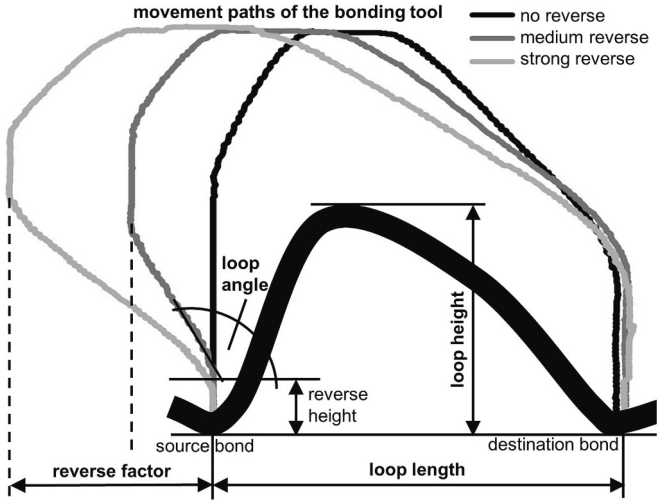

Fig. 1. Loop forming process with the parameters influencing the reverse movement [8].

hardness [5–7]. On the other hand, a possible backward movement during loop forming process causes the heel to be bent and thus plastically deformed [8]. Depending on the selected wire material, the process specific bonding parameters may lead to cracking and failure of the wire bonds as a consequence of the weakening of the heel region.

The overall reliability of the semiconductor power devices is assessed by active and passive thermal life tests. Depending on the testing conditions, the modules fail mainly due to wire bond failure or solder fatigue. The quality of wire bonds with regard to heel cracking and lift-off failure is usually evaluated by pull or shear tests [3]. However, these static test methods do not correspond to the actual loading conditions that occur in operation. Currently research is going on to establish efficient cyclic mechanical test procedures that reproduce these failure scenarios in a realistic and accelerated manner [8–11]. This allows a quick and targeted evaluation and screening of the weak sites without having to test the entire module through time-consuming temperature cycling tests. Reduction of the testing time is achieved by increasing the testing frequency which may vary from a few Hz up to kHz range. With regard to wire bond heel failure, a number of mechanical fatigue test procedures have been proposed. Ramminger et al. [12] used a displacement-controlled fatigue testing setup to study heel crack failures in Al wire bond loops. The set-up allowed cyclic lateral displacements of one bonding area relative to the other in the loop direction with excitation amplitudes of up to about 50 µm. Based on the experimental results and finite element simulations a Coffin Manson type fatigue life model was presented. Further, it was found that the heel cracking is strongly dependent on the loop geometry. A similar low cycle mechanical loop cycle test (LCT) was used by Merkle et al. [13] based on which a lifetime prediction model for heavy Al wire bonds in the low cycle regime has established. In a study by Czerny et al. [14] a displacement controlled accelerated mechanical fatigue testing setup working at 500 Hz was used to study the effect of bond geometry on fatigue failure of Al bonds as a result of heel cracking. It was suggested that loop height and angle have the largest influence on the fatigue life of wire bonds. Recently, a highly accelerated mechanical fatigue testing technique was used for evaluation of high cycle fatigue behavior of wire bond loops [8]. The study was conducted by using the BONDTEC BAMFIT tester in a modified form which is originally designed for rapid qualification of the bond interfaces [11]. The BAMFIT (Bond accelerated mechanical fatigue interconnect testing) method which works at a testing frequency of 60 kHz utilizes specially designed resonance gripping-tweezers to induce cyclic shear stresses in the bonding interface which lead to fatigue failure due to bond wire lift-off. Accordingly, lifetime curves with a large number of data points can be obtained in a very short time. In order to induce heel cracks by this testing system, the wire is pinched by the gripping-tweezers at a height of ~1 mm along the wire loop. During the excitation, due to back-and-forth movement of the wire at very low amplitudes below 1 µm, the heel region is subjected to cyclic bending loads which results in propagation of fatigue cracks and failure of the wire bond due to heel cracking. Using this testing technique allowed to study the impact of reverse movement during the bonding process on the lifetime of Al wire bonds [8].

In this work the effect of geometry and loop forming parameters on the quality and lifetimes of wire bonds prepared with Al wires of different hardness were studied. The investigations were carried out by using two different accelerated mechanical lifetime tests, surface roughness measurements to evaluate the wrinkling of the heel area by laser confocal microscopy, and static pull tests. Fatigue tests were conducted by a displacement controlled low cycle mechanical fatigue test for wire bond loops comparable to the one described in [7] and the modified BAMFIT method [8]. Moreover, the initial appearance of the heel region, the degree of wrinkling of the bonds and the damage sites subsequent to fatigue tests were investigated by optical methods. Subsequently, the results of pull test and wrinkling measurements are correlated to the lifetime and discussed.

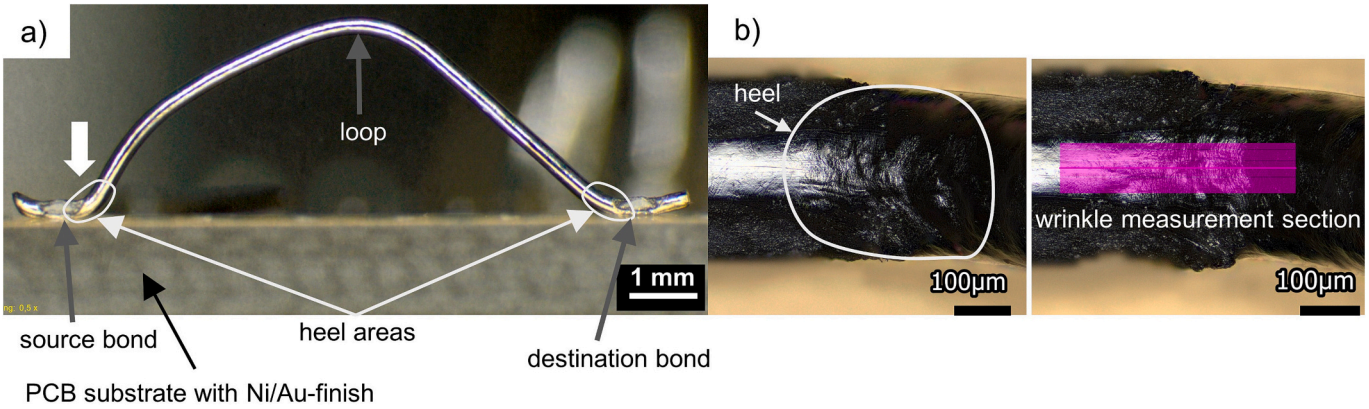

Fig. 2. Characteristics of the wire bond on the example of a 300 µm wire, according to [4]:
a) side view of the wire bond with labeled parts, wide arrow indicates the position where image in (b) is taken,
b) top view of the source bond, marked is the heel area (left, white) and the area, where surface roughness measurements have been made (right, purple).

Table 1
Mechanical specifications of the investigated aluminum wires.

Wire material	Diameter (µm)	Elongation (%)	Breaking load (cN)
AluBond Pure H11	300	>5	280–430
AluBond Prime H14CR Soft	300	>10	320–420
AluBond Prime H14CR Medium	300	>15	450–650

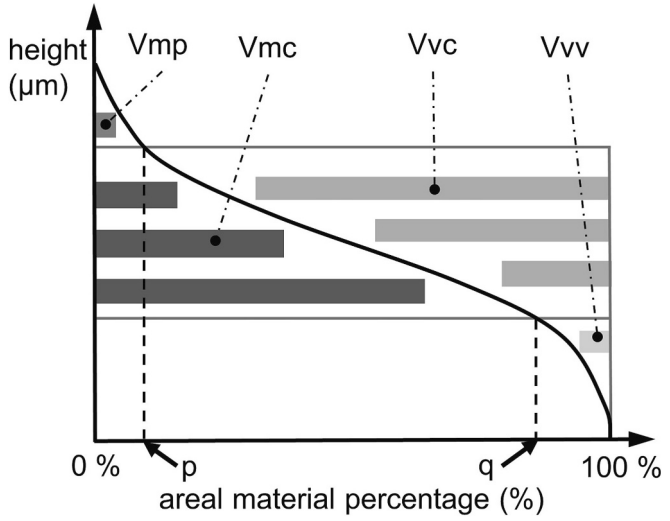

Fig. 3. Abbott-Firestone curve with the volume parameters [17], $p = 10$ %, q = 80 % [19].

2. Experimental investigation

2.1. Specimen

2.1.1. Material

In this investigation wire materials of different qualities were used in order to determine the impact of initial plastic deformation on their fatigue behavior. In Table 1 the wire materials under test and their mechanical specifications are given. All wires were bonded with a Delvotec M17S bonding machine, the AluBond Pure H11 wire was additionally bonded with a Hesse BJ939 bonding machine.

The used substrate materials are a PCB with Ni/Au finish (Ni thickness (4.7 ± 0.2) µm and Au thickness (70 ± 5) nm) and a Ni plated Al sheet (Ni thickness (10 ± 3) µm).

2.1.2. Bond and loop parameters

The experiments were conducted on aluminum wire bonds of 300 µm diameter with an overall same loop geometry. The loop lengths of the wire bonds were set to 5 mm and 8 mm, which resulted in loop heights of 2 mm and 3 mm, respectively.

Shear tests together with deformation measurements were used to optimize the bonding process parameters, bond force and ultrasonic energy, according to Technical Bulletin DVS 2811 [4]. For each wire-substrate combination separate optimized bonding parameters were identified. All further investigations used these parameters in which the loop forming parameters were varied. In order to attain a different intensity of bending and thus prestressing in the heel area, the reverse movement was set to different levels by varying the bonding machine parameters reverse factor (M17S, given in percent) and loop angle (BJ939, given in degree). These parameters are shown in Fig. 1, with the movement path of the bonding tool in gray, and the resulting wire geometry in black. The approach to obtain the exact movement path of the bonding tool is described elsewhere [15].

2.2. Test methods

2.2.1. Wrinkling measurements in the heel area

In order to quantify the wrinkling as a result of the reverse movement in the loop forming process and the mechanical aging, surface roughness in the heel area was measured with confocal laser scanning microscopes (Keyence VK-X1100 and Olympus Lext OLS4000). On the right side in Fig. 2 b, the positioning of the wrinkle measurement section for a 300 µm wire is shown with a usable measuring distance along the heel of 400 µm.

The details of wrinkling measurement method are given in [15], where the arithmetic mean values of the roughness profiles (Ra) and greatest heights of the roughness profiles (Rz) have been evaluated [16]. In contrast to [15], the present work uses the more appropriate volume parameters, which describe to which proportion the investigated volume is filled with material or voids [17]. These parameters are the volume material peak (Vmp), the volume material core (Vmc), the volume void core (Vvc) and the volume void valley (Vvv). They are defined by the Abbott-Firestone curve (Fig. 3), which represents the areal material percentage as a function of the measuring height [17,18]. The higher the ordinate moves, the less material surface intersects the surface laid along the measuring area. Either the empty or filled volume below or above the height coordinate is then related to this area, which

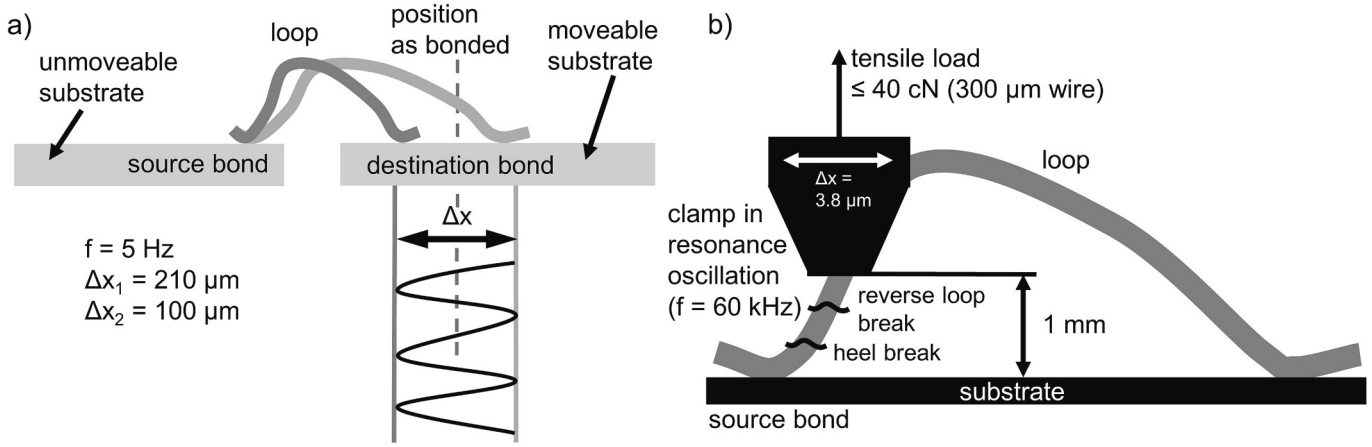

Fig. 4. Mechanical accelerated lifetime tests carried out:
a) cycle test (LCT),
b) BAMFIT technique (the positions of the breaks are explained later in Section 3.2).

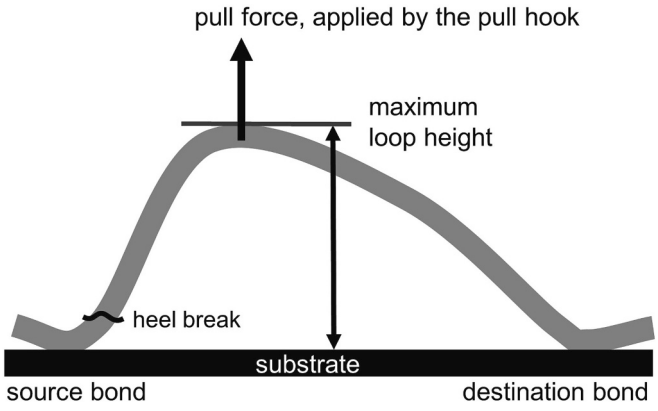

Fig. 5. Pull test setup.

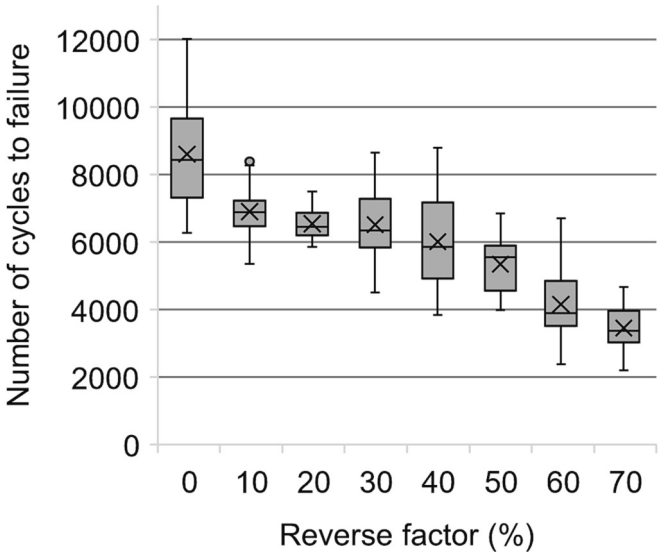

Fig. 6. Results of the LCT (amplitude 210 µm, f = 5 Hz), AluBond Prime H14CR Medium (d = 300 µm, *n* = 30), PCB substrate with Ni/Au-finish (Boxplot).

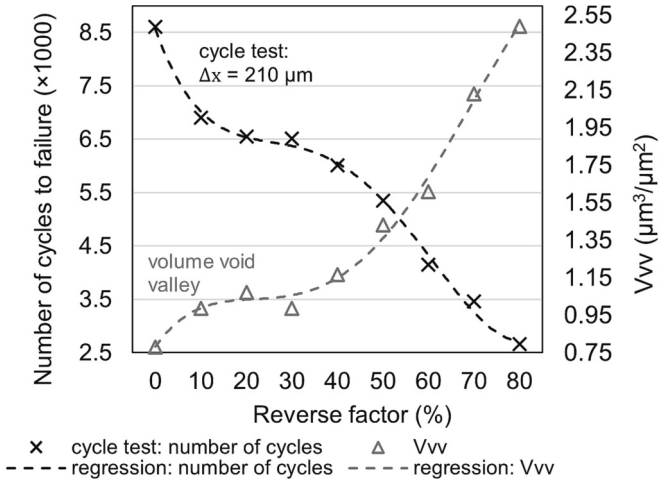

Fig. 7. Comparison of the wrinkling (Vvv, averages, Keyence VK-X1100) with the lifetime from the LCT (averages); AluBond Prime H14CR Medium (300 µm), PCB substrate with Ni/Au-finish, loop length 8 mm. The lines are polynomial fits and are only a guide to the eye.

is why the parameters have the unit volume per area. The Abbott-Firestone curve is therefore very suitable for the characterization of the heel area, since it covers both surface and volume properties and breaks down into four different sub-parameters that analyze different characteristics. Lifetime data can be compared with the four parameters to find out with which parameter the lifetime values correlate most closely and then find explanation approaches for this in conjunction with fracture patterns.

Observations show visible surface changes in the heel area after the initial plastic deformation during the bonding process. To determine and correlate the different wrinkling measurement values to the lifetime and/or material properties, two mechanical accelerated lifetime tests with regard to heel fracture and a conventional pull test were conducted.

2.2.2. *Mechanical accelerated lifetime tests*

Two different lifetime testing methods with different elongation and frequency of the cyclic load have been carried out by means of accelerated mechanical testing. Fig. 4 a illustrates the principle of the mechanical loop cycle test (LCT) (comparable to the setup in Ref. [7]), in which the wire bond is alternately stretched and compressed in the loop direction with an amplitude Δx at a constant frequency of f = 5 Hz by moving the substrate with the destination bond in a linear direction while the substrate with the source bond remains fixed. The sample is mounted such that the zero point of the oscillation represents the situation as bonded. The Δx has been varied between 100 and 210 µm in different test runs. Fig. 4 b depicts the concept of a modified BAMFIT technique [8], in which the gripping tweezers which clamp the wire are excited to ultrasonic oscillations. As mentioned before, in contrast to the BAMFIT test, where the clamp is placed directly on the bonding wedge close to the substrate, in the modified BAMFIT test the clamp is placed at a height of 1 mm at the loop and stresses the heel. With 60 kHz, the frequency in the BAMFIT is about 12,000 times as high as in the LCT, while the excitation amplitude is about 25 to 60 times smaller with its 3.8 µm for 300 µm wire.

2.2.3. *Pull test*

Destructive pull tests (at the XYZtec Condor Sigma with pull parameters according to [4]) were performed in the initial state of the wire bonds and after applying certain cyclic loading in the LCT. It was carried out to identify the fracture mechanism under a tensile load for the generated loop geometry. In order to reveal correlations, the measured data from the pull tests as well as from the wrinkling measurements were compared with the lifetime values from the LCT.

Fig. 5 shows the principle of the pull tests carried out. The pull force is applied by the pull hook and is positioned at the maximum height of the loop. The loop angles used to calculate the correction factors for the pull forces were measured for each r. f. using non-destructive pull tests (according to [4]).

3. Results

3.1. *LCT, wrinkling measurements and pull tests: AluBond Prime H14CR Medium (d = 300 µm, loop length = 8 mm), PCB substrate with Ni/Au-finish*

Low cycle fatigue tests resulted in heel fracture at the source bonds. Fig. 6 shows the number of cycles until failure (N_f) as a function of the reverse factor (r. f.) for the AluBond Prime H14CR Medium wire bonds. In this case, an amplitude of 210 µm has been set in the LCT. The global maximum is located at factor 0 %, where no reverse movement has taken place. At reverse factors between 10 and 30 % the results show a local plateau followed by a continuous decrease after 40 %.

These results have been compared with the results of the wrinkling analysis of 20 specimens, which is shown in Fig. 7. The volume void valley (Vvv) in the heel area of the initial state of the bonds behaves inversely to N_f as a function of the reverse movement.

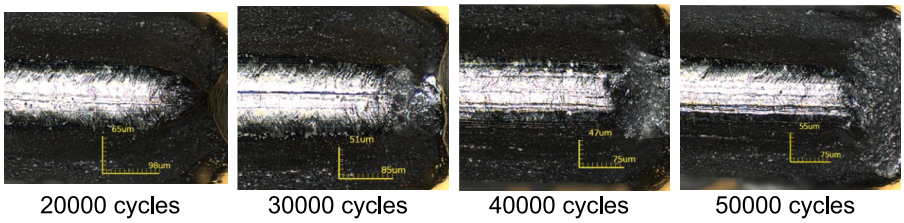

Fig. 8. Heel at the source bond after the pull test depending on the number of cycles from the LCT (Δx = 100 µm), AluBond Prime H14CR Medium (d = 300 µm, r. f. 0 %), PCB substrate with Ni/Au-finish.

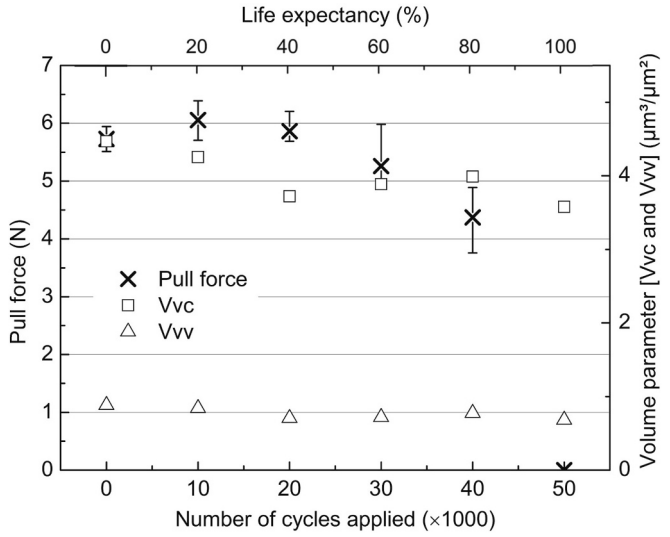

Fig. 9. Results of the pull tests and the wrinkling measurements (Olympus OLS4000, averaged volumetric parameters) as a function of loading cycles of LCT (Δx = 100 µm), AluBond Prime H14CR Medium (d = 300 µm, r. f. 0 %), PCB substrate with Ni/Au-finish. The average pull force is given by the cross, whereas the bars indicate the maximum and minimum values of the measured sample set.

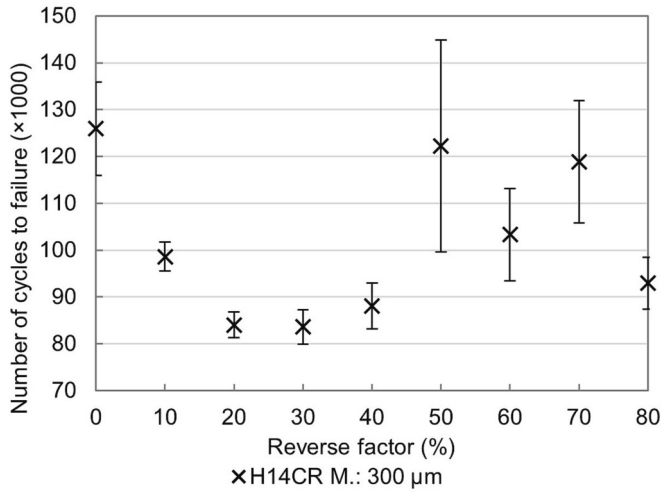

Fig. 10. Results of BAMFIT (amplitude 3.8 µm), AluBond Prime H14CR Medium (d = 300 µm, loop length = 8 mm), PCB substrate with Ni/Au-finish. The bars represent the 95 %-confidence interval of the averages.

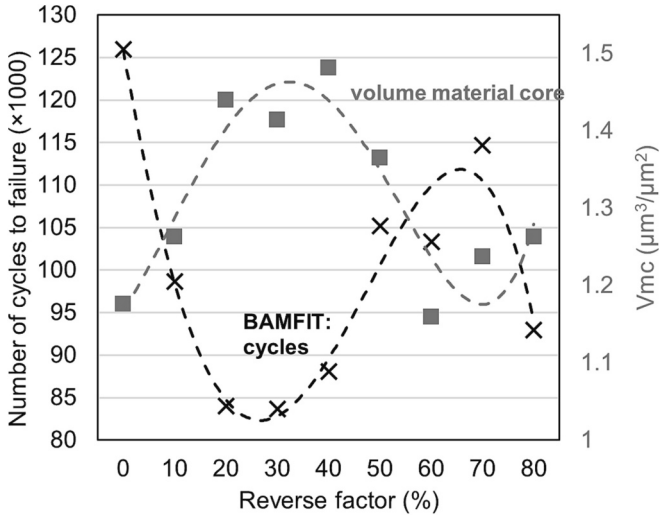

Fig. 11. Correlation of the wrinkling (Vmc, averages, laser scanning microscope VK-X1100) with the lifetime from the BAMFIT (averages); AluBond Prime H14CR Medium (d = 300 µm), PCB substrate with Ni/Au-finish, loop length 8 mm. The dashed lines show a polynomial fit and are only a guide to the eye.

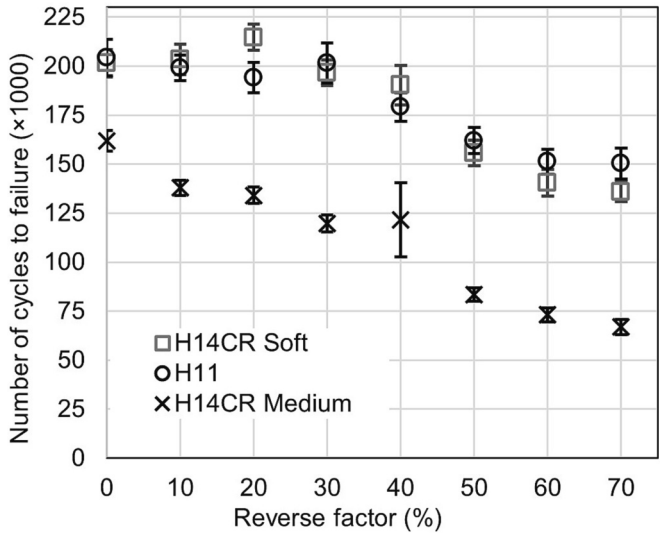

Fig. 12. Results of BAMFIT (amplitude 3.8 µm) for wire bonds of three different materials (loop length = 5 mm, n = 28 to 50), Ni plated Al substrate [8], (US = ultrasonic energy, BF = bond force); the bars represent the 95 % confidence interval of the averages.

In order to investigate the degradation behavior of the heel area during the LCT, the loops were loaded up to a certain number of cycles at a constant amplitude of 100 µm. Subsequently the samples which revealed different degrees of damage were subjected to pull tests and wrinkling investigations. Five different sample sets were prepared from 10,000 cycles up to 50,000 cycles in steps of 10,000, which is approx. 20 % of the expected lifetime. For each of the 5 sample sets, pull force and roughness values (sample set size n = 5 to 10) were measured and

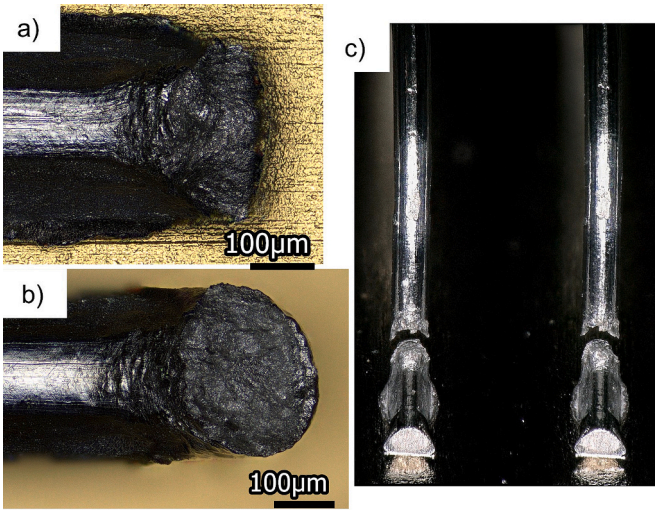

Fig. 13. Broken wires in the top view (a, b) and side view (c) (AluBond Prime H14CR Medium, d = 300 µm, r. f. 30 %, PCB substrate with Ni/Au-finish) a) LCT; b, c) BAMFIT.

compared with the values from the initial (uncycled) state as shown in Fig. 9. It can be seen, that during the first 20 % of the life expectancy, the pull forces increase slightly. From 20 to 40 %, the forces and the roughness parameters decrease slightly. Pure ductile fractures appeared in these phases after the pull test. After 40 % of the life expectancy, the forces start to decrease significantly and the fracture patterns change (Fig. 8). They were only ductile on the outer side, while on the inside, fatigue fracture behavior was already visible.

The proportion of fatigue fracture grows with increasing load (Fig. 8). After 80 % of life expectancy, the parameter volume void core (Vvc) increases, compared with 60 % life expectancy, to drop again at the end.

3.2. BAMFIT and wrinkling measurements

The BAMFIT and wrinkling measurements were done at two different sample sets (a and b), explained in detail in the following.

a) AluBond Prime H14CR Medium (d = 300 µm), loop length = 8 mm, PCB substrate with Ni/Au-finish.

Similar to LCT, heel failure occurred at the source bond after BAMFIT. The fatigue fracture is observed at the heel and the reverse loop just above the heel at the location of largest plastic deformation caused by the bonding process. On a few bonds the fatigue fracture starts to propagate at the heel or the reverse loop but finally breaks near the grips. This type of failure mode was not evaluated, since the N_f of multiple crack paths would lead to misleading results. The positions of the fracture sites vary with the reverse factor and are marked in Fig. 4. The results of the modified BAMFIT tests for the AluBond Prime H14CR Medium wire bonds with diameters of 300 µm are shown in Fig. 10. For the loop length of 8 mm (sample size $n = 35$ to 50), the N_f decreases from the initial state until 20 % r. f. and then gradually increases reaching nearly the initial state values at 50 % and then drops again after 70 %. The global minimum at about 30 % can be linked to a distinct shift in the failure mode. It was observed, that up to 20 % r. f. only heel crack failures and above 30 % only fractures in the reverse loop occurred which seem to result in higher N_f.

In a similar fashion as in Fig. 7, the lifetime data have been compared with the wrinkling values ($n = 20$) in the initial state of the heel plotted in Fig. 11. The BAMFIT results and the Vmc evaluation of the wrinkling measurements correlate very well with an inverse relationship to each other.

b) AluBond Prime H14CR Medium/Soft/AluBond Pure H11 (d = 300 µm, loop length = 5 mm), Ni plated Al substrate.

In a further series, 300 µm wire bonds made of three different wire materials have been compared in the BAMFIT test. All of them were bonded on the Ni plated Al substrate with a loop length of 5 mm. The number of cycles to failure as a function of r. f. is plotted in Fig. 12. The lifetime data of the H11 and H14CR Soft wire bonds are taken from [8]. These softer wires, which have been bonded with the same bonding parameters, reach similar N_f values. The N_f values remain at the initial state up to r. f. of 30 % and then decrease at higher r. f. The wire bonds made of harder AluBond Prime H14CR Medium, have significantly lower lifetime values and decrease almost constantly with increasing r. f. The bond parameters differ only slightly.

The data from Fig. 12 were also compared with the wrinkling values from the initial measurements of the heel of the wire bonds. Again, inverse correlations as in Fig. 11 could be recognized. This consolidates the finding, that the Vmc and the lifetime in BAMFIT almost behave inversely.

3.3. Fracture patterns as a result of cycle test and BAMFIT

The fracture patterns resulting from the mechanical fatigue tests have been compared. For this purpose, the broken bond contacts were observed from above and geometrically measured (microscope VK-X1100, sample size $n = 6$). As a result of the LCT, Fig. 13 a, the heel is broken close to the wedge. The 300-µm wire samples failed in BAMFIT test predominantly further away from the heel at the bent section straight through the wire shown in Fig. 13 b and Fig. 15 c, where the maximum vertical height of the fracture in the LCT (approx. 280 µm) is slightly lower than in the BAMFIT (approx. 310 µm).

The differences in the fracture position are predominantly due to the differences in the loading conditions of the two testing methods. A finite element analysis (FEA) was conducted to compare the stress distribution of the loading conditions of the LCT and BAMFIT test according to Fig. 4. As for this comparison the first few cycles of a mechanical simulation at the maximum respected excitation amplitude with the same mesh size of 50 µm and multilinear kinematic hardening material model for the entire Al wire. The FEA results depict the von Mises stress distribution in the cross section of the heel region at Δx of 210 µm of the destination pad in the LCT test in Fig. 14 a and 3.8 µm at the wire grippers 1 mm above the fixed source pad in Fig. 14 b. The stress distribution shows an upwards shift in the stress concentration of the BAMFIT test compared to the LCT and that in the LCT test the stress concentration on the bottom side of the wire is more pronounced and the distance between stress concentration on the topside and bottom side is much shorter compared to the stress distribution of the BAMFIT rest. Hence the crack propagation in the LCT tend to start from both sides closer to the heel, whereas in the BAMFIT test the fatigue crack propagates more likely in the bent region slightly above.

Metallographic cross-sections were prepared along the loop direction of the wedge and the heel area. Fig. 15 a shows the cross-section of the initial state of a heel, where the heavily deformed zone and the resulting changes in the local grain structure due to the strong reverse movement are visible (marked with a circle). This type of wrinkling is also visible at the wire surface in Fig. 2 b, where the heel area is marked.

Fig. 15 b shows an example of the heel fracture as a result of LCT, while Fig. 15 c displays a heel break caused by BAMFIT for 300 µm bond wires. Fig. 15 also reveals differences in the fracture pattern in the cycle test (b) comparing to the BAMFIT (c) in these exemplary images. While the fatigue crack grows almost at the same location in both cases, as the cross section of the wire gradually decreases, the final failure occurs due to rupture of the wire loop from the wedge in BAMFIT test.

4. Discussion

First of all, it should be noted that even in the initial state there are clearly different surface properties in the heel area, depending on the

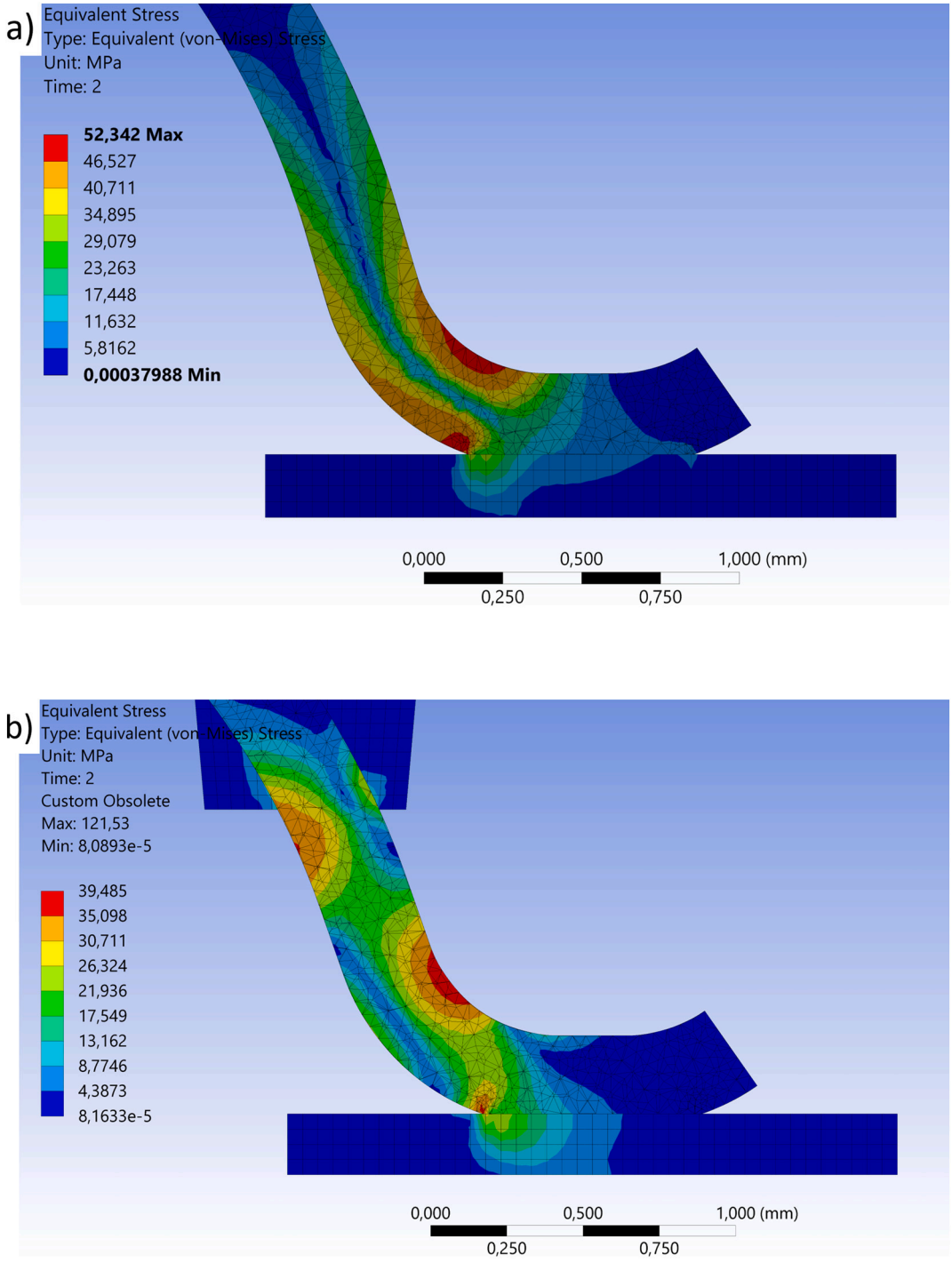

Fig. 14. FEA von Mises stress distribution in the heel region at the respected maximum excitation amplitude of the a) LCT and b) BAMFIT test.

applied r. f. Fig. 7 and Fig. 11 show clear changes for the initial Vvv and Vmc values, respectively. However, the measurements of the wrinkling values at different degrees of degradation (cycle numbers) show that these initial values then change only minimally during plastic deformation in the mechanical cycle tests. On the other hand, however, there are clear anti-correlations between these values and the lifetime cycle numbers determined in the LCT and in BAMFIT, Fig. 7 and Fig. 11. Therefore, it can be assumed that the r. f. leads to a lasting change of the material. This concerns especially the microstructure in the heel area, which is particularly stressed during loading due to the loop geometry. This change in the microstructure is also directly confirmed by the visible finer local grain structure in the cross section, Fig. 15. The slight increase of the pull forces up to 10,000 cycles in the mechanical test with simultaneous slight decrease of the Vvc and Vvv values can thus also be attributed to a test-related microstructural change (work hardening), which is small compared to the effect of the cold deformation of the material in the heel caused by the reverse movement. Moreover, the Vvv can be considered as a measure of the size of the notches [17], the increase of which reduce the lifetime in the cycle test, Fig. 7.

Despite the same pre-damage caused by bonding with r. f., a closer look reveals in certain cases a different fracture pattern during LCT compared to BAMFIT. Both the height and the final angle of the crack path are different, Fig. 15. Furthermore, an examination of the fracture surfaces, Fig. 13, leads to the conclusion that with the BAMFIT there is a

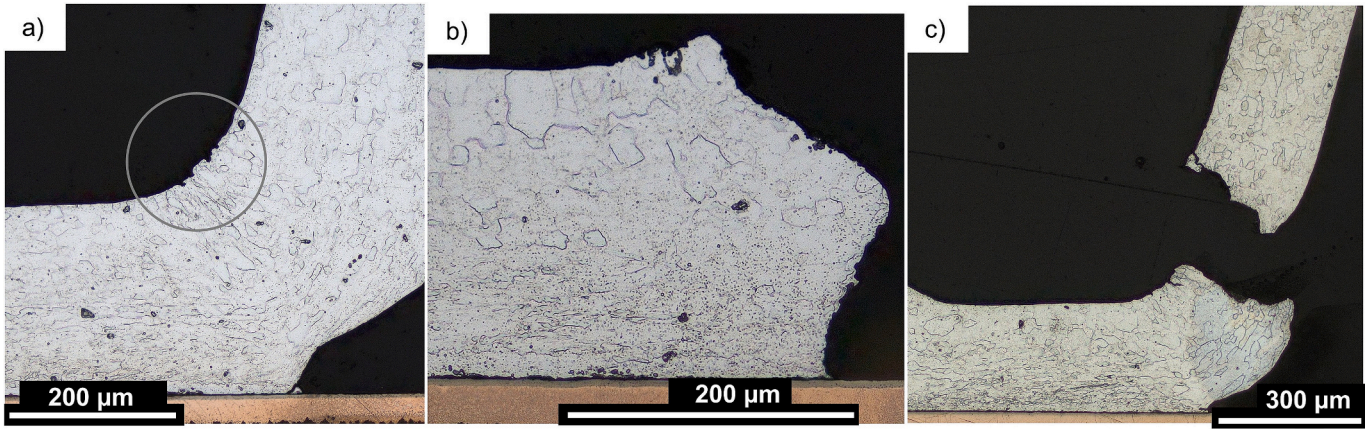

Fig. 15. Cross-sections of the heel area (AluBond Prime H14CR Medium, d = 300 µm, PCB substrate with Ni/Au-finish)
a) initiaI, reverse factor 70 %,
b) fracture after the LCT, reverse factor 30 %,
c) fracture after the BAMFIT, reverse factor 30 %.

flat fatigue zone followed by a ruptured remaining wire, while the cyclic mechanical test shows a ductile fracture pattern in most cases. Therefore, it is most likely that the fracture mechanism, and thus the fracture progress and speed, will differ between the two cyclic loading methods. In addition, the number of cycles in LCT (e.g., with 210 µm deflection in Fig. 6) of ≤10,000, compared to BAMFIT (>100,000 cycles, Fig. 10) and its deflection in the order of <10 µm, are about 10 to 20 times lower. This finding can be explained by the fact that, first of all the load geometry is different in BAMFIT. It is applied quite close to the source bond and thus there is only a short steeply rising piece of the loop between the oscillating gripper and the later fracture point. In the LCT, on the other hand, the entire loop is compressed and stretched, thus distributing the movement over the entire length of the loop. This deformation of the entire geometry changes the force applied to the heel. Another crucial difference is the frequency used. With mechanical cycling at 5 Hz, the slow movement leads to work hardening. This also leads to the slightly increasing pull force values in Fig. 9 for the low cycle numbers. These very local zones of work-hardened material, together with the loop and linear motion in the test, then lead to a situation that results in crack growth with mechanical pulling apart of the material. Another comparison between lifetimes under the two test methods was made with wire of different hardness. While the H11 and the H14CR Soft belong to the softer wires, the harder H14CR medium has an approx. Doubled breaking load and a more than doubled elongation, Table 1. In the tests of the wires with both aging methods, Fig. 12, the same decreasing behavior of the curves as a function of r. f. can be seen for all materials. First, however, it is noticeable that the curve for the harder material is shifted. In the case of BAMFIT, Fig. 12, significantly lower lifetimes (cycle numbers) were measured. A drop to about a quarter of the values for the soft wire is present. Whereby the soft wires behave very similarly to each other and do not have to be considered separately. In the case of LCT, on the other hand, the soft wire, considered over the various r. f., achieves in the best case only about half N_f of the hard wire. As above, it can be argued here, that the fracture mechanism driven by BAMFIT benefits from a stiffer connection between the gripping point of the gripper and the fracture site at the heel. In case of the soft pure aluminum H11 wire is subjected to cyclic hardening, due to the local excitation of the wire near the heel region in the BAMFIT test, which results in a higher fatigue resistance in the high cycle regime [20]. In the case of the longer-lasting hard wires in the LCT, it can be speculated that the overall force effect changes in favor of the harder material, since the entire loop geometry is always included in this test and the load at the later damage site results from this and the material properties. Furthermore, it should be mentioned that the soft and hard wires were bonded with different bonding parameters, namely in the optimum of the respective determined bonding parameter ranges (according to [4]). As a result, the initial local material properties in the heel area may also deviate slightly.

The reason for the difference in the lifetime curves of Fig. 10 and Fig. 12 can be the different loop geometry (loop lengths of 5 and 8 mm), since the reduced loop length of the bonds on the Ni-plated Al substrate also means that the loop height is smaller and the inclination angles of the loop change. The different bonding parameters on Ni plated Al or Ni/Au PCB substrate may have another impact on the fatigue results, as more bonding force and less ultrasonic energy was used to contact the bonds on the Ni plated Al than on the PCB substrate with Ni/Au finish, which could lead to slightly different hardness values of the heel regions.

Apart from the discussed differences in the results depending on the cyclic loading method, general statements regarding the influence of the r. f. on the service life can be made from the results. Lifetimes are only slightly affected at moderate r. f. values, but drop significantly for values >30 % r. f., Fig. 6 and Fig. 12.

Furthermore, for a statement about material changes introduced during bonding, which have a negative effect on the service life, a consideration of the wrinkling measurements seems to provide a better correlation, Fig. 7 and Fig. 11. This can be explained by the fact that the deformations on the wire surface, which are quantified by the wrinkling measurements, reflect the local stress better than a machine parameter, which only characterizes the travel of the bonding head (cf. Fig. 1), although the real wire deformation is still influenced by other parameters, such as the wire hardness and also other geometrically effective machine parameters (time of wire clamp opening, heights of the points when changing the direction of the bonding head, etc.).

5. Conclusion

In this paper, two different accelerated lifetime testing methods for Al heavy wire bonds based on mechanical stresses have been compared: the LCT and the BAMFIT technique. The obtained lifetime data, the results of wrinkling measurements and pull tests were compared to detect correlations. These correlations facilitate predictions about the expected life span. Equal wire bonds have performed differently in the lifetime tests. Nevertheless, significant factors affecting the lifetime could be identified. With regard to loop forming process, it has been proven that a slight reverse movement should not be exceeded in order to ensure high lifetime values in both the LCT and the BAMFIT. With respect to the wire type, it was demonstrated that the softer wire bonds made of AluBond Pure H11 and AluBond Prime H14CR Soft with the

diameter of 300 µm reached higher lifetime values in the BAMFIT than those made of harder AluBond Prime H14CR Medium. While no correlations of lifetime values to pull test results are visible, two relationships between lifetime and wrinkling ratings were identified. Low Vvv values in the heel of the unloaded bonds indicate increased lifetime values in the LCT, while low Vmc values in the heel indicate higher lifetime values in the BAMFIT.

Further detailed microstructural investigations and failure analysis of the wires subsequent to LCT and BAMFIT tests would be beneficial for a better understanding of the degradation process in comparison to field application failure. FEM analysis might provide more information about the correlation of the damage parameters at the heel and the bond process parameters. It would then also be possible to determine whether qualitative information about the wire bond lifetime could be obtained from Vvv and Vmc in a non-destructive manner. Finally, by combining the results of both measurement methods, it would then be possible to make reliable statements about the service life of the wire bonds in a simple manner.

Competing interests statement

The authors would like to state that there are no competing interests, neither financial nor personal.

CRediT author statement

Florens Felke: Investigation, Writing - Original Draft, Visualization, Formal analysis, Validation. **Anne Groth:** Writing - Review and Editing, Supervision, Resources, Conceptualization, Data analysis. **Martin Hempel:** Writing - Review and Editing, Methodology, Data analysis. **Bernhard Czerny:** Writing - Review and Editing, Methodology, Investigation. **Torsten Döhler:** Investigation, Methodology, Formal analysis. **Ute Geissler:** Writing - Review and Editing, Supervision, Project administration, Resources, Conceptualization. **Golta Khatibi:** Writing - Review and Editing.

Data availability

The experimental data can be requested from the authors.

Acknowledgements

The project was supported by the BMBF, grant number 13FH057PX6, the DFG-Fraunhofer-Industrial trilateral project AlCuBo, grant number Fraunhofer 059-602027/DFG MU 2963/25-1, and the company F&K Delvotec Bondtechnik. Further thanks go to the companies xyztec and Heraeus for providing equipment.

References

[1] C. Durand, M. Klingler, D. Coutellier and H. Naceur, “Power cycling reliability of power module: a survey,” IEEE Trans. Device Mater. Reliab., vol. 16, no. 1, pp. 80–97, Mar. 2016, doi: https://doi.org/10.1109/TDMR.2016.2516044.

[2] E. Arjmand, P. A. Agyakwa, M. R. Corfield, J. Li, and C. M. Johnson, “Predicting lifetime of thick Al wire bonds using signals obtained from ultrasonic generator,” IEEE Trans. Compon. Packag. Manuf. Technol., vol. 6, no. 5, pp. 814–821, Apr. 2016, doi:https://doi.org/10.1109/TCPMT.2016.2543001.

[3] G. Harman, Wire Bonding in Microelectronics, 3rd ed, McGraw Hill, 2010.

[4] Merkblatt DVS 2811, Prüfverfahren für Drahtbondverbindungen: DVS, Ausschuss für Technik, Arbeitsgruppe "Fügen in Elektronik und Feinwerktechnik", DVS - Deutscher Verband für Schweißen und verwandte Verfahren e.V., Feb. 2017.

[5] U. Geißler, M. Schneider-Ramelow, K.-D. Lang, H. Reichl, Investigation of microstructural processes during ultrasonic wedge/wedge bonding of AlSi1 wires, IEEE J. Electron. Mater. 35 (1) (2006) 173–180, https://doi.org/10.1007/s11664-006-0201-2.

[6] U. Geißler, H.-J. Engelmann, I. Urban, H. Rooch, FIB preparation and TEM analytics on AlSi1 bond pads, Prakt. Metallogr. 43 (10) (2006) 520–532.

[7] L. Merkle, T. Kaden, M. Sonner, A. Gademann, J. Turki, C. Dresbach, M. Petzold, Mechanical fatigue properties of heavy aluminium wire bonds for power applications, in: 2008 2nd Electronics System Integration Technology Conference, Greenwich, 2008, pp. 1363–1368, https://doi.org/10.1109/ESTC.2008.4684554.

[8] H.-G. von Ribbeck, T. Döhler, B. Czerny, G. Khatibi, U. Geißler, Loop formation effects on the lifetime of wire bonds for power electronics, in: CIPS 2020; 11th International Conference on Integrated Power Electronics Systems, Berlin, Germany, Mar. 2020.

[9] G. Khatibi, B. Czerny, A. Lassnig, M. Lederer, J. Nicolics, J. Magnien, E. Suhir, A novel approach for evaluation of material interfaces in electronics, in: 2016 IEEE Aerospace Conference, Big Sky, MT, USA, 2016, pp. 1–11, https://doi.org/10.1109/AERO.2016.7500758.

[10] B. Czerny, G. Khatibi, Accelerated mechanical fatigue interconnect testing method for electrical wire bonds, Tech. Mess. 85 (4) (2018) 213–220, https://doi.org/10.1515/teme-2017-0131.

[11] B. Czerny, G. Khatibi, Highly accelerated mechanical lifetime testing for wire bonds in power electronics, J. Microelectron. Electron. Packag. 19 (2) (2022), https://doi.org/10.4071/imaps.1717134.

[12] S. Ramminger, N. Seliger, G. Wachutka, Reliability model for Al wire bonds subjected to heel crack failures, Microelectron. Reliab. 40 (2000) 1521–1525, https://doi.org/10.1016/S0026-2714(00)00139-6.

[13] L. Merkle, M. Sonner, M. Petzold, Lifetime prediction of thick aluminium wire bonds for mechanical cyclic loads, Microelectron. Reliab. 54 (2) (Feb. 2014) 417–424, https://doi.org/10.1016/j.microrel.2013.10.009.

[14] B. Czerny, I. Paul, G. Khatibi, M. Thoben, Experimental and analytical study of geometry effects on the fatigue life of Al bond wire interconnects, Microelectron. Reliab. 53 (2013) 1558–1562, https://doi.org/10.1016/j.microrel.2013.07.090.

[15] T. Döhler, H.-G. von Ribbeck, F. Fidorra, F. Felke, U. Geißler, Study of the Wrinkle Formation in the Heel Zone of Heavy Wire Bonds, in: 2020 43rd International Spring Seminar On Electronics Technology (ISSE), Demanovska Valley, Slovakia, 2020, pp. 1–6, https://doi.org/10.1109/ISSE49702.2020.9121156.

[16] Geometrical Product Specifications (GPS), Surface Texture: Profile Method – Terms, Definitions and Surface Texture Parameters (ISO 4287:1997 + Cor 1:1998 + Cor 2:2005 + Amd 1:2009); German Version EN ISO 4287:1998 + AC:2008 + A1:2009, DIN EN ISO 4287, DIN-Normenausschuss Technische Grundlagen (NATG), Berlin, Jul. 2010.

[17] Geometrical Product Specifications (GPS), Surface Texture: Areal – Part 2: Terms, Definitions and Surface Texture Parameters (ISO/DIS 25178-2:2019); German and English version prEN ISO 25178-2:2019, German Standard DIN EN ISO 25178-2 (Entwurf), DIN-Normenausschuss Technische Grundlagen (NATG), Berlin, Feb. 2020.

[18] J. Niedermeier, A. Kopp, P. Dincsoy, B. Bold, T. Bernthaler, G. Schneider, Mikroskopische charakterisierung der ‘wrinkle-bildung’ bei aluminium-stromkollektorfolien von Li-ionen-batterien, Metallographie-Tagung (Sep. 2020) 183–188.

[19] Geometrical Product Specifications (GPS), Surface Texture: Areal – Part 3: Specification Operators (ISO 25178-3:2012); German Version EN ISO 25178-3: 2012, Deutsche Norm DIN EN ISO 25178-3, DIN-Normenausschuss Technische Grundlagen (NATG), Berlin, Nov. 2012.

[20] S. Suresh, Fatigue of Materials, Cambridge University Press, 1991.